Rock Mechanics and Rock Engineering (2023) 56:6157–6166
https://doi.org/10.1007/s00603-023-03345-9

TECHNICAL NOTE

Reliability Assessment of Empirical Equations, ANN and MARS Models for Predicting the Mode I Fracture Toughness from Non-destructive Rock Properties

Abiodun Ismail Lawal[1,2] · **Sangki Kwon**[1]

Received: 12 August 2022 / Accepted: 16 April 2023 / Published online: 24 May 2023

Highlights

- Mode I fracture toughness is highly imperative in various rock mechanics applications.
- Machine learning models are proposed for accurate prediction of mode I fracture toughness.
- The reliability assessment of the empirical equations and proposed models enables the selection of the most suitable among them.
- The reliability analysis revealed that some of the models assessed are unsuitable for fracture toughness prediction.

Keywords Fracture toughness · Empirical equations · Machine learning · Normality test · Reliability analysis

1 Introduction

Accurate measurement of mode I fracture toughness is of great importance in rock mechanics applications such as slope stability analysis, tunnel excavation and rock fragmentation including blasting and hydraulic fracturing (Whittaker et al. 1992; Feng et al. 2017; Roy et al. 2018). According to the literature, mode I fracture toughness could be considered as a characterization of geomaterials, rock fragmentation index and the material property for stability analysis and modelling (Franklin et al. 1988; Afrasiabian and Eftekhari 2022). To measure the mode I fracture toughness, various laboratory procedures including the chevron bend and shot rod (ISRM 1988), Brazilian disc method (Guo et al. 1993; Atkinson et al. 1982; Xu and Fowell 1994) and semicircular bend method (Kuruppu et al. 2014; Wang et al. 2021) have been developed. Other advanced experimental methods such as cracked chevron-notched Brazilian disc (CCNBD), hollow centre cracked disc (HCCD), straight notch disk bend (SNDB), chevron notch semi-circular bend (CNSCB) and single edge crack round bar bending (SECRBB) among others have been used to measure the rock fracture toughness in different modes (Chang et al. 2002; Amrollahi et al. 2011; Pakdaman et al. 2019). However, the laboratory experiment for K_{IC} determination is generally too tedious and time consuming coupled with the requirement of high level of expertise as compared to other mechanical properties such as compressive and tensile strengths (Zhixi et al. 1997; Kahraman and Altindag 2004; Ke et al. 2008).

Apart from the laboratory means of determining K_{IC}, other methods like conventional numerical, analytical and empirical methods have been used to predict the K_{IC} (Chen et al. 2001; Eftekhari et al. 2015a,b; 2017). The analytical and numerical methods are said to be one-to-one mapping models depicting that detailed geometric and physical mechanisms are required which make them rigorous, tedious, computationally expensive and requiring some assumptions (Jing 2003; Sakellariou and Ferentinou 2005; Lawal and Kwon 2021). Their results also diverge from the experimental results on some occasions, as their veracity depends

✉ Sangki Kwon
kwonsk@inha.ac.kr

[1] Department of Energy Resources Engineering, Inha University Yong-Hyun Dong, Nam Ku, Incheon, Korea

[2] Department of Mining Engineering, Federal University of Technology, Akure, Nigeria

on how good the boundary assumptions are (Lawal and Kwon 2022). Although the laboratory experiment if conducted properly remains the most reliable or viable means of K_{IC} determination, the quick estimation of K_{IC} may be needed during the routine design of mines and also many laboratories that are void of the K_{IC} equipment may also require the estimation of K_{IC} for the design purpose. As a result, researchers have developed some empirical models for the estimations of K_{IC} (Chang et al. 2002; Zhang 2002; Zhixi et al. 1997, etc.). The models are sometimes the correlation between the K_{IC} and physical or mechanical properties, while those that combined different properties of rocks are also available. However, the accuracy of the empirical equations is usually low. Machine learning (ML) models have also been used for accurate prediction of K_{IC} (Roy et al. 2018; Afrasiabian and Eftekhari 2022). The major drawback of the ML models is the unavailability of the tractable mathematical form that can be easily implemented (Afrasiabian and Eftekhari 2022). The recently proposed ML model by Afrasiabian and Eftekhari (2022) is in the mathematical form, but the performance of their model is low.

Despite the availability of different advanced methods for the K_{IC} predictions, field engineers seem to prefer empirical equations to the complex methods without minding the accuracy. Although, some empirical equations have shown a very high R^2 value that is greater than 90%, most importantly those that were based on the acoustic rock properties and density. Hence, it will be important to assess the reliability of the existing empirical equations to assist in quick selection of the most suitable one among the scattered equations, as the reliability of the scattered empirical equations for K_{IC} prediction is yet to be evaluated by any researcher. Therefore, we assess the reliability of the existing empirical models, the proposed MARS- and ANN-based models in this study using the experimental database compiled from previous studies. This will serve as a guide to the users of the scattered equations for K_{IC} predictions in the literature and therefore the proposed study is novel and useful in rock mechanics applications.

2 Methodology

2.1 Data Compilation and Explanation

The adopted datasets are compiled from scattered experimental datasets in the literature. The adopted datasets comprised the non-destructive rock properties such as acoustic rock properties and rock density together with the K_{IC}. The datasets are about forty-three (43) in total as presented in Table 1. The P-wave velocity (V_P), S-wave velocity (V_S) and rock density (ρ) are the model-independent variables, while K_{IC} is the dependent variable. The correlations between these datasets are presented in Fig. 1. The model predictors' correlations with K_{IC} are relatively good based on the confidence ellipses set at 95% confidence interval. This is also supported by coefficient of determinations (R^2) shown in Fig. 1. The correlation between rock density and K_{IC} seems to be the weakest as revealed by the big confidence ellipse and low R^2 value. The correlation between V_S and V_P is the highest, as the size of the confidence ellipse is narrower. The bigger the confidence ellipse, the weaker is the correlation. These geomaterial properties, that is, V_P, V_S and ρ are used as the model parameters, as the procedures required in determining them are not cumbersome and not destructive.

2.2 Literature Equations

In this study, some of the available empirical equations for the prediction of K_{IC} are extracted from the literature. About eighteen (18) equations which considered single independent variables were obtained, while three multi-independent variable equations were also obtained from different literature (Table 2). However, out of the 18 empirical equations and three multi-parameters equations, only about nine (9) equations which utilized single parameter were subjected to reliability evaluation alongside with the newly proposed ML-based models in this study. The reason for excluding some of the models in Table 2 is on the bases of the parameters used in developing those equations, which are not considered in some of the obtained dataset for this study. The excluded equations comprised at least one destructive rock property. The exclusion is imperative to enhance fair comparison/evaluation. The models based on non-destructive properties also revealed good performance and are more realistic in the sense that they can be measured alongside with K_{IC} on a single core sample unlike the destructive rock properties such as UCS and σ_t, which require separate rock core sample preparation for their determination. This implies that more samples will be needed, which is also costly and time consuming to prepare separate core samples for K_{IC} and other destructive property predictions. There could be a slight disparity in the core samples characteristic even if obtained from the same rock mass. Hence, the selected non-destructive properties, apart from the fact that they are not difficult to measure, are also more realistic, because the same sample used in determining them is also used for the K_{IC} test (which is also a destructive rock property).

2.3 Assessments of Equations

The assessment of the obtained equations in the literature and the proposed models in this study was performed using the collated data presented in Table 1. To compare the *predictions* of the assessed models and the measured data points, the root mean square error (RMSE), mean absolute error

Table 1 Adopted database for the reliability assessment

SN.	References	K_{IC} (MPa.m$^{0.5}$)	V_P (m/s)	V_S (m/s)	ρ (g/cm^3)
1	Zhixi et al. (1997)	0.25	1806.2	1443.7	2.318
2		0.27	1869.2	1351.4	2.200
3		0.35	1744.7	1385.1	2.266
4		0.51	2526.9	1702.9	2.568
5		0.45	2054.1	1666.7	2.468
6		0.65	4601.2	2654.9	2.621
7		0.47	2500	1666.7	2.175
8		0.71	2718.1	1947.1	2.368
9		0.75	3142.9	2135.9	2.53
10		0.56	3083.3	1953.1	2.509
11		0.55	4258.9	2453.1	2.622
12		0.8	2948.7	2090.9	2.567
13		0.77	2804.9	1982.8	2.487
14		0.75	2941.2	2127.7	2.459
15		0.63	4163	2455.1	2.653
16		0.72	2825	2260	2.435
17		1.1	4125	2690.2	2.744
18		0.63	3609.4	2357.1	2.526
19		0.6	2620.2	1919	2.535
20		0.51	3288.5	2758.1	2.588
21		0.6	3850.2	2315.5	2.603
22		0.54	3680.3	2100.2	2.597
23		0.36	3120	1700	2.114
24		0.3	1780	2600	2.212
25		1.1	2860	2300	2.579
26		0.78	3410	2010	2.515
27		2	5000	3200	2.5
28		1.2	4000	2900	2.5
29		3.5	5920	3760	2.551
30		3.14	5190	3780	2.3
31		3.19	5980	3800	2.9
32	Muñoz-Ibáñez et al. (2020)	0.4	2634	1818	2.2
33		1.46	3686	2563	2.5
34		1.34	4100	2562	2.6
35		0.12	2920	1510	2.1
36	Chang et al. (2002)	0.73215	3104.453	1883.721	2.56106
37		1.06506	3402.055	1978.056	2.69006
38		1.34793	3731.103	1852.276	2.72131
39		1.00486	4388.074	2510.371	2.62154
40		2.03479	4936.112	2478.926	2.68101
41		1.42916	5624.529	2948.352	2.75054
42		1.79254	6188.289	3042.686	2.84937
43		2.26688	6360.112	3042.686	2.85848

(MAE), coefficient of determination (R^2), and p value from Mann–Whitney test were adopted. Thereafter, the most suitable model is selected. The adopted approach in assessing the most reliable model in this study is similar to that of Mohammed et al. (2019). They selected a reliable model for UCS prediction in their study. After the selection of a suitable model in this study, the selected model(s) is(are) further correlated with the measured value.

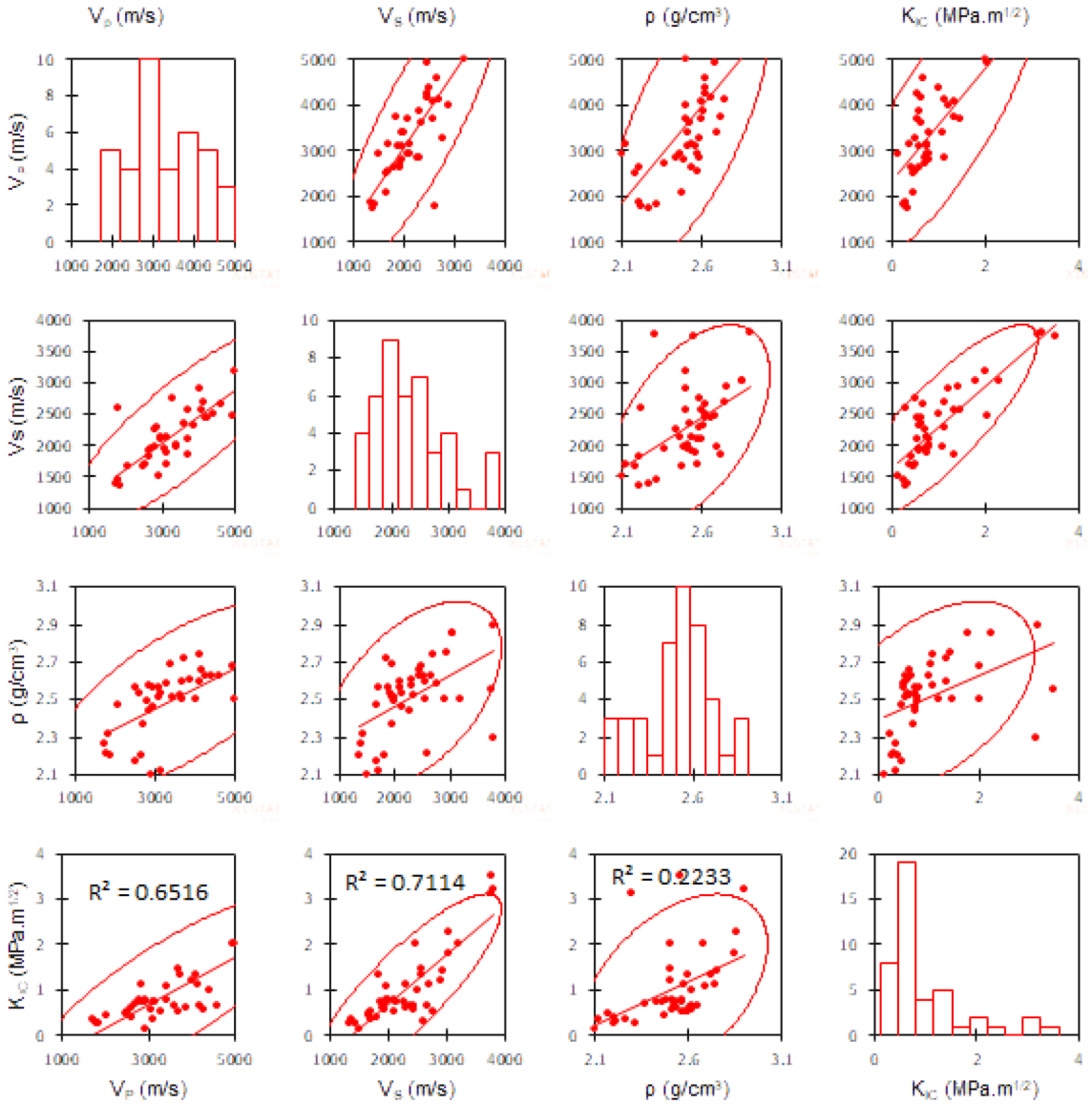

Fig. 1 The scattered correlation plots of the datasets

2.4 Model Development and Statistical Examinations

2.4.1 MARS

Multivariate adaptive regression spline (MARS) proposed by Friedman (1991) is a non-parametric regression method that enables the capturing of the nonlinear relationships between the data by assessing the knots in the manner similar to the step functions. MARS builds the model using the sum of the weighted basis functions. The basis function can be of three forms: the constant which is always a single term, a hinge function and product of two or more hinge functions. The hinge function is of the form max(0,x-c) or max(0,c-x) (Lawal et al. 2021) and it is very paramount as it is the part that captures the nonlinearity in the data. To build the MARS model, there are two stages, the forward and backward stages. Many candidate basis functions are generated in pairs in the forward stage. Each of the generated pair of the functions is added if it minimizes the overall error of the model. The required number of functions that the model generate can be controlled with hyperparameters. In the backward stage, the generated basis functions are pruned and only those

Table 2 Obtained literature equations

Eq. no.	Material	Equations	R^2	References
1	Sandstone	$K_{IC} = 0.000361V_P - 0.332$	0.92	Zhixi et al. (1997)
2	Sandstone	$K_{IC} = 0.0006147V_s - 0.5517$	0.90	Zhixi et al. (1997)
3	Shale	$K_{IC} = 5.4074 \times 10^{-5}V_P + 0.3876$	0.56	Zhixi et al. (1997)
4	Shale	$K_{IC} = 0.0001021V_s + 0.3490$	0.64	Zhixi et al. (1997)
5	Granite and marble	$K_{IC} = 3.5 \times 10^{-4}V_P - 0.18$	0.64	Chang et al. (2002)
6	Granite and marble	$K_{IC} = 7.1 \times 10^{-4}V_S - 0.29$	0.44	Chang et al. (2002)
7	Different rock types	$K_{IC} = 0.45V_P - 0.58$	0.55	Roy et al. (2017)
8	Different rock types	$K_{IC} = 0.9V_S - 1.06$	0.6	Roy et al. (2017)
9	Different rock types	$K_{IC} = 3.21\rho - 6.95$	0.91	Brown and Reddish (1997)
10	Different rock types	$K_{IC} = 0.0037e^{0.0022\rho}$	0.54	Roy et al. (2017)
11	Granite and marble	$K_{IC} = 4.28 \times 10^{-3}\sigma_c + 1.05$	0.55	Chang et al. (2002)
12	Granite and marble	$K_{IC} = 6.23 \times 10^{-3}E + 1.23$	0.21	Chang et al. (2002)
13	Granite and marble	$K_{IC} = 2.45SG - 5.19$	0.51	Chang et al. (2002)
14	Granite and marble	$K_{IC} = -0.5\mu + 1.7$	0.60	Chang et al. (2002)
15	Different rock types	$K_{IC} = \left(\frac{\sigma_t}{6.88}\right)^{1/0.62}$	0.94	Zhang (2002)
16	Different rock types	$K_{IC} = \sigma_t + 2.35/9.35$	0.62	Whittaker et al. (1992)
17	Different rock types	$K_{IC} = \left(\frac{\sigma_t}{8.88}\right)^{1/0.62}$	0.94	Zhang et al. (1998)
18	Different rock types	$K_{IC} = 0.11\sigma_t + 0.23$	0.62	Roy et al. (2017)
19	Different rock types	$K_{IC} = 0.024\sigma_c - 0.48(\sigma_c < 145\text{MPa})$ $K_{IC} = 0.01\sigma_c - 0.2(\sigma_c > 145\text{MPa})$	0.69 0.65	Roy et al. (2017)
20	Different rock types	$K_{IC} = 0.09\sigma_t + 0.15V_P + 0.13V_S - 0.49$	0.83	Roy et al. (2018)
21	Different rock types	$K_{IC} = 0.297 + 0.003\sigma_c + 0.023\sigma_t + 0.008E$	0.74	Afrasiabian and Eftekhari (2022)
22	Different rock types	$G_1 = \left(\sin(0.33)/\sigma_c \times E\right)\ln(\sigma_t \times E - 18.8)$ $G_2 = -3.99 - \text{atan}[1.28 - \sigma_t - \sin(\sigma_t)]$ $G_3 = \frac{1}{\ln(44.37\sin(E)+\sigma_c-13.99)-8.3}$ $G_4 = (\sin(E) - E)(-6.27 - \sigma_t) - (7.59E \times \cos(E))$ $K_{IC} = G_1 - G_2 - G_3 - G_4$	0.83	Afrasiabian and Eftekhari (2022)

that add to the performance of the model are allowed to remain while others are deleted. The deletion is achieved with the generalization cross-validation (GCV) score. The key advantage of the MARS model over other machine learning approaches is the ability to present its results in the form of simple equation. Apart from this, it can be developed with limited data sets just like the linear regression, which the MARS model leveraged on to capture the nonlinearity in the data. The proposed MARS model was built in the MATLAB with the rock non-destructive properties as the input, while the K_{IC} was the only targeted output. The number of bases function was set to 7 at the forward phase, but the number of bases functions of the final model was pruned to 5 at the backward phase (Fig. 2). The obtained MARS using the piecewise-linear model is presented in Eq. (23).

$$MARS_{K_{IC}} = 0.93712 + 4.7523BF1 - 1.3373BF2 - 94.7414BF3 + 12.7223BF4, \quad (23)$$

where

$$BF1 = \max\left(0, V_S^n - 0.49481\right),$$

$$BF2 = \max\left(0, 0.49481 - V_S^n\right),$$

$$BF3 = \max\left(0, 0.51573 - V_P^n\right),$$

$$BF4 = \max(0, \rho^n - 0.58375).$$

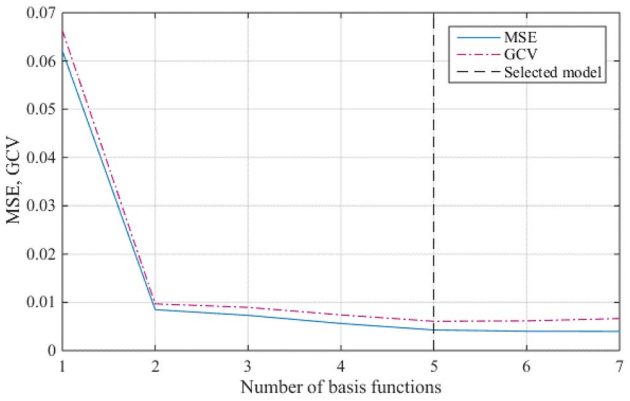

Fig. 2 The generalization cross-validation (GCV) score with number of basis functions

2.5 Artificial Neural Network

ANN can arguably be said to be the most adopted machine learning method. It has been used to solve a wide range of problems across all the fields of human endeavour. The ANN model is adopted in this study, as it has not been widely used in predicting the K_{IC} and none of the existing study that utilizes ANN for K_{IC} makes available the implementable code for the practical implementation of the ANN model. The proposed ANN in this study was developed using the gathered data presented in Table 1. The dataset is enough for the development of ANN model, as several ANN models have been developed in the past using 27, 30, 34 and 38 datasets (Dehghan et al. 2010; Ebrahimi et al. 2015; Akinwekomi and Lawal 2021; Aladejare et al. 2022) that are below the number of datasets used in this study. The adopted datasets are pre-processed through normalization to ensure data uniformity and avoid overfitting. The ANN model was implemented in the MATLAB using a self-iterated approach. The number of neurons in the input layers are three, which are V_P, V_S and density, while the number of neurons in the output layer is one, which is K_{IC}. The number of neurons in the hidden layer was varied between two and ten and the results obtained for the training and testing stages with the overall performance are presented in Table 3. The network with nine neurons in the hidden layer outperformed the others and therefore was selected as the optimum network (Fig. 3). The weights and biases extracted from the selected network are transformed into the implementable MATLAB code as presented in Appendix A for easy K_{IC} prediction.

2.6 Statistical Analyses and Hypotheses Test

The values of K_{IC} were predicted for the empirical models developed based on non-destructive rock properties using the mined datasets from the literature (Table 1). Afterwards, the RSME, MAE and R^2 in Eqs. (24–26) were computed for the predicted and measured data points. Thereafter, the normality test was conducted on the measured and predicted K_{IC} using the MiniTab software. Based on the outcome of the normality test, the statistical test was selected. For the non-normal datasets, the p value of each empirical equation was considered using non-parametric Mann–Whitney test. The procedures adopted for the statistical test is as suggested by Mohammed et al. (2019) and presented in Fig. 4.

$$RMSE = \sqrt{\frac{\sum_{i=1}^{n}\left(Y_{meas} - Y_{pred}\right)^2}{n}}, \tag{24}$$

$$MAE = \frac{\sum_{i=1}^{n} abs\left(Y_{meas} - Y_{pred}\right)}{n}, \tag{25}$$

Table 3 Different simulated ANN structures

	Training	Testing	Overall	RMSE*	ME
3-2-1	0.93462	0.895565	0.94174	0.15834	0.00857
3-3-1	0.94372	0.922575	0.96649	0.12173	− 0.00765
3-4-1	0.98419	0.971625	0.98079	0.09201	0.00071
3-5-1	0.9858	0.991595	0.98695	0.07596	0.00685
3-6-1	0.99817	0.94532	0.99305	0.05590	− 0.00522
3-7-1	0.99692	0.999305	0.99751	0.03318	0.00116
3-8-1	0.99728	0.99412	0.99557	0.04452	0.00425
3-9-1	0.99892	0.99896	0.99849	0.02584	− 0.00094
3-10-1	0.9978	0.99851	0.99824	0.02790	0.00088

*RMSE and mean error (ME) are obtained from MATLAB simulations with normalized overall datasets

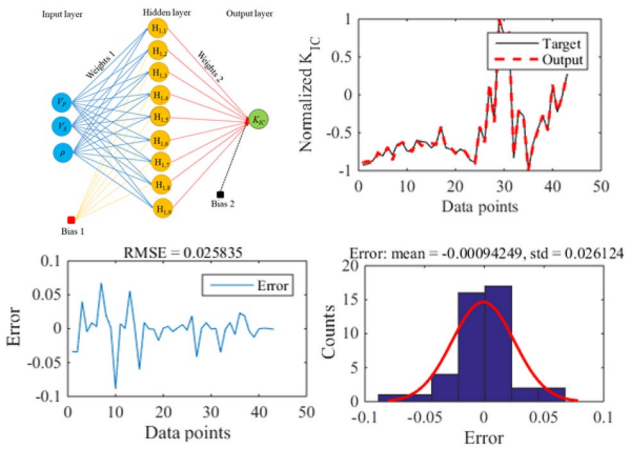

Fig. 3 Selected ANN structure with the performances

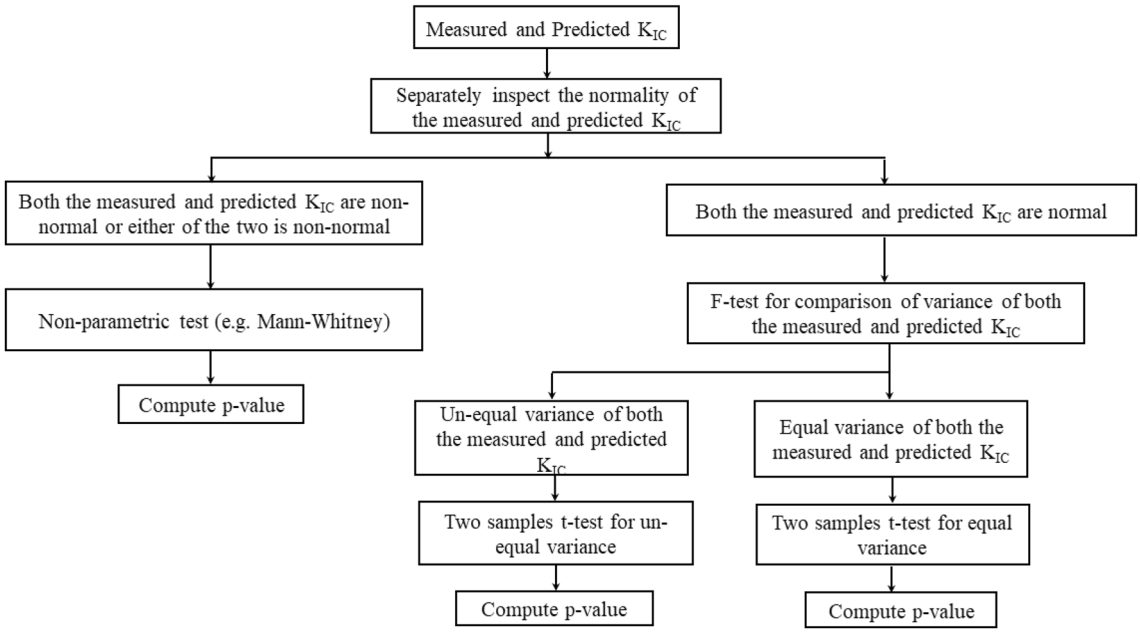

Fig. 4 Framework of the adopted methodology (after Mohammed et al. 2019)

$$R^2 = 1 - \frac{\sum_{i=1}^{n} \left(Y_{meas} - Y_{pred}\right)^2}{\sum_{i=1}^{n} \left(Y_{meas} - \overline{Y}_{meas}\right)^2}, \tag{26}$$

where Y_{meas} and Y_{pred} are the measured and predicted K_{IC}, while $\overline{Y}_{meas}$ is the mean of the measured K_{IC} and n is the number of data points.

A two-tailed test with 95% confident interval was used with test hypothesis assumptions, null hypotheses and research hypotheses. For the null hypotheses, Ho measured and predicted data are identical, while for the research hypotheses, Ha measured and predicted data are not identical. During the statistical analysis, Ho was accepted for p value $>=0.05$, and Ho was rejected for p value <0.05 for all tests.

3 Results and Discussion

The reliability of empirical equations and the proposed models was assessed using the adopted database of acoustic properties, rock density and K_{IC} to compute the RMSE, MAE and R^2 between the measured and predicted values as presented in Table 4. From Table 4, the minimum RMSE and MAE are 0.0437 (for ANN) and 0.0259 (for ANN),

Table 4 Evaluation criteria for K_{IC} compared to measured data

Models	Evaluation criteria		
	R^2	RMSE	MAE
ANN	0.997	0.043661	0.0259
MARS	0.884	0.272891	0.186879
Equation (1)	0.6516	0.511615	0.332054
Equation (2)	0.7114	0.536541	0.341465
Equation (3)	0.6516	0.858844	0.517969
Equation (4)	0.7114	0.857621	0.520884
Equation (5)	0.6516	0.519735	0.371721
Equation (6)	0.7114	0.592378	0.522204
Equation (7)	0.6516	0.478385	0.328601
Equation (8)	0.7114	0.442142	0.315287
Equation (9)	0.2233	0.748169	0.553687

Table 5 Mann–Whitney test for the K_{IC} modes compared to measured data

Models	Normality test		Normality test for error distribution	p value from Mann–Whitney test
	Measured	Predicted		
ANN	< 0.005	< 0.005	< 0.005	0.972
MARS	< 0.005	< 0.005	0.007	0.931
Equation (1)	< 0.005	0.064	< 0.005	0.262
Equation (2)	< 0.005	0.143	< 0.005	0.776
Equation (3)	< 0.005	0.064	< 0.005	0.006
Equation (4)	< 0.005	0.143	< 0.005	0.008
Equation (5)	< 0.005	0.064	< 0.005	0.029
Equation (6)	< 0.005	0.143	< 0.005	0
Equation (7)	< 0.005	0.064	< 0.005	0.204
Equation (8)	< 0.005	0.143	0.011	0.294
Equation (9)	< 0.005	0.035	< 0.005	0.075

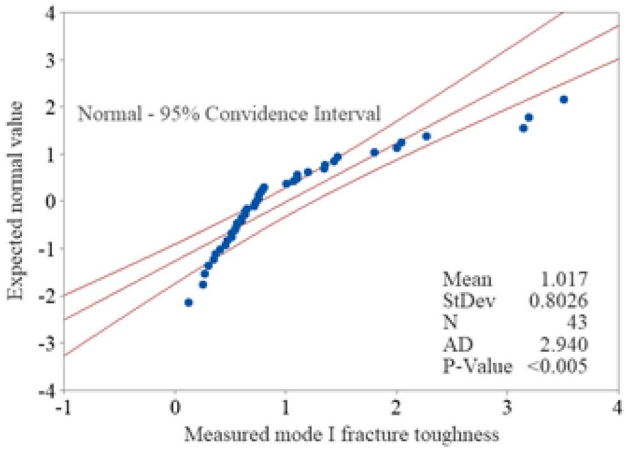

Fig. 5 Probability plot of the measured K_{IC}

respectively, while their respective maximum values are 0.8588 (Eq. (3)) and 0.5537 (Eq. (9)), respectively. The maximum R^2 value was 0.997, obtained for the ANN model, while the minimum R^2 is 0.2233 obtained for Eq. (9).

For the accuracy assessment of the models, RMSE is more suitable than MAE when the distribution of the error (that is the difference between the measured and predicted values) is normally distributed (Chai and Draxler 2014). However, MAE can as well be used where two models have similar RMSE values and different MAE values. In this study, all the error distributions, as presented in Table 5, are not normally distributed, as their p values are less than 0.05. Therefore, RMSE will be misleading in assessing the reliability of the models and hence not considered (Chai and Draxler 2014). Also, MAE is not also considered in evaluating the suitability of the models because of its correlation with RMSE. In addition, R^2 value is also a weak indicator and not considered as well (Willmott and Matsuura 2005). The results in Table 4 reveal that RMSE and MAE may give misleading assessment, because their values for RMSE and MAE are considerably small and all the models are suitable for the assessment of K_{IC}, thanks to the detailed statistical study conducted to further probe into the effectiveness of these equations in K_{IC} predictions.

The statistical outcomes of the measured and predicted K_{IC} by ANN, MARS and Eq. (9) are non-normal, while that of the predictions by Eqs. (1–8) are normal, as their p values are greater than 0.05. The Mann–Whitney test was conducted to check the reliability of the models, since both measured and predicted or either one of the two is required to be non-normally distributed as shown in the chart (Fig. 5). The normal probability plot of the measured value is presented in Fig. 5, while the normal probability values of the models are presented in Table 5.

The p values obtained from Mann–Whitney test conducted on the pair of measured and predicted values by the models are also presented in Table 5. The minimum and maximum p values are 0 and 0.972, respectively. The p values obtained revealed that out of the models subjected to the reliability analysis, ANN, MARS and Eqs. (1, 2, 7, 8, 9), have p values greater than 0.05. Since the higher the p value, the better is the model based on the conducted test, ANN, MARS and Eq. (2) are most suitable for the prediction of

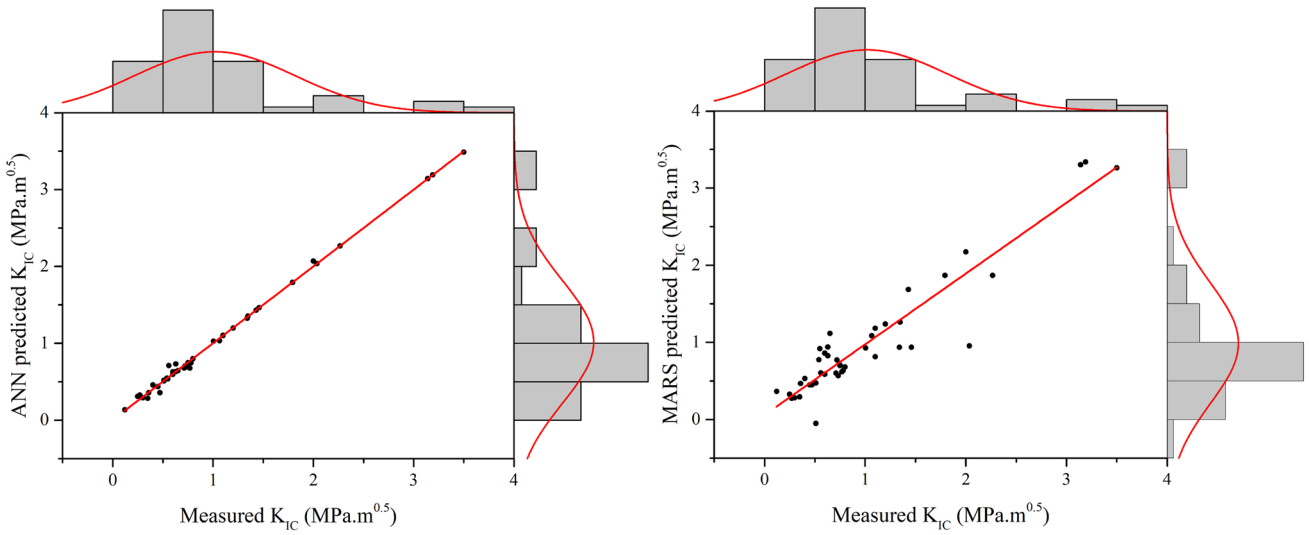

Fig. 6 Correlation between the measured and predicted values of the most reliable models

K_{IC} and can be used with more confidence, while Eqs. (3, 4, 5 and 6) should not be used.

The correlation plot of the measured and the predicted values using the ANN and MARS models, the most suitable models, are shown in Fig. 6. It can be seen that the prediction of the ANN model is actually close to the measured values. The histogram of the ANN model is closely related to that of the measured data. Similarly, the MARS model prediction also revealed a close predictions to the measured K_{IC}, but not as that of the ANN model. In fact, the histogram of the MARS model differs from that of the measured K_{IC}.

4 Conclusion

This study assessed the reliability of various empirical models for K_{IC} predictions alongside with two machine learning methods, ANN and MARS models, with practical implementation insight using the mined data in the literature. To achieve this, each of the selected empirical equations based on the available data were re-evaluated alongside with the two newly proposed ML models. They are then subjected to strong statistical tests beyond the usual RMSE, MAE and R^2 statistical indicators. The normality tests were first conducted on the measured data, equations and the error in the MiniTab software with two different hypotheses to accept or reject the model. The non-parametric statistical examination was then used to select the most suitable model. The outcomes of the study revealed that ANN, MARS and Eq. (2) are found to be the most suitable for the prediction of K_{IC} and can be used with more confidence, while Eqs. (3, 4, 5 and 6) should not be used. The traditional indicators (RMSE, MAE and R^2) should be used with caution, as they can give misleading information about the models. This type of study is highly imperative to ensure that an appropriate model is used for rock mechanics application with outmost confidence.

Appendix A

MATLAB codes for implementing the ANN model

```
%Inputs
V_P = input('V_P:');V_S = input('V_S:');rho = input('rho:');
%Normalization
V_Pn = 2*(V_P-1744.7)/4615.412–1; V_Sn = (2*(D2-1351.4)/2448.6)-1; rhon = 2.5*(rho − 2.1)− 1;
%ANN functions
x1 = − 6.06366032460768*tanh(0.895121158*V_Pn + 8.167572732*V_Sn + 3.944227813*rhon-2.58309722218044);
x2 = 4.53201670500747*tanh(0.196052392*V_Pn + 2.600267977*V_Sn + 9.176464667*rhon-5.00433781940571);
x3 = 2.880302002207 96*tanh(1.309774377*V_Pn + 3.341374862*V_Sn-0.977837086*rhon + 5.1535124737128);
x4 = 8.026958694425 21*tanh(2.404311328*V_Pn + 1.567524559*V_Sn-3.024444841*rhon − 1.40852079842265);
x5 = −2.92338426677153*tanh(3.058872395*V_Pn + 10.63463327*V_Sn + 0.959284589*rhon + 1.22980599592424);
x6 = -0.5456373575971 29*tanh(− 0.679478982*V_Pn + 0.369334148*V_Sn-0.300141158*rhon-0.82346245277411);
x7 = 1.5406348640654 2*tanh(−3.048599 26*V_Pn -8.357267272*V_Sn-0.198463676*rhon-3.12285508892506);
x8 = 2.20382967656225*tanh(−3.026260943*V_Pn-2.9724508*V_Sn + 8.859728745*rhon + 3.718036624176 4);
x9 = 5.6911107157675*tanh(0.806341017*V_Pn + 5.510536647*V_Sn + 0.734720571*rhon + 0.588796585443898);
KIC_ANN_norm = tanh(x1 + x2 + x3 + x4 + x5 + x6 + x7 + x8 + x9 + 1.46999477925268);
KIC_ANN = 1.69*KIC_ANN_norm + 1.81.
```

Acknowledgements This work was supported by the Inha University Research Grant (2023).

Data availability Not applicable.

Declarations

Conflict of Interest The authors declare that they have no known competing financial interests or personal relationships that could have appeared to influence the work reported in this paper.

References

Afrasiabian B, Eftekhari M (2022) Prediction of mode I fracture toughness of rock using linear multiple regression and gene expression programming. J Rock Mech Geotech Eng. https://doi.org/10.1016/j.jrmge.2022.03.008

Akinwekomi AD, Lawal AI (2021) Neural network-based model for predicting particle size of AZ61 powder during high energy mechanical milling. Neural Comput & Applic 33:17611–17619

Aladejare EA, Ozoji T, Lawal AI, Zhang ZX (2022) Soft computing-based models for predicting the characteristic impedance of igneous rock from their physico-mechanical properties. Rock Mech Rock Eng. https://doi.org/10.1007/s00603-022-02836-5

Amrollahi H, Baghbanan A, Hashemolhosseini H (2011) Measuring fracture toughness of crystalline marbles under modes I and II and mixed mode I-II loading conditions using CCNBD and HCCD specimens. Int J Rock Mech Min Sci 48(7):1123–1134

Atkinson C, Smelser RE, Sanchez J (1982) Combined mode fracture via the cracked Brazilian disk test. Int J Fract 18(4):279–291
Brown G, Reddish D (1997) Experimental relations between rock fracture toughness and density. Int J Rock Mech Min Sci 34(1):153–155
Chai T, Draxler RR (2014) Root Mean Square Error (RMSE) or Mean Absolute Error (MAE)?–Arguments Against Avoiding RMSE in the Literature. Geosci Model Dev 7(3):1247–1250
Chang SH, Lee CI, Jeon S (2002) Measurement of rock fracture toughness under modes I and II and mixed-mode conditions by using disc-type specimens. Eng Geol 66(1):79–97
Chen F, Sun Z, Xu J (2001) Mode I fracture analysis of the double-edge cracked Brazilian disk using a weight function method. Int J Rock Mech Min Sci 38(3):475–479
Dehghan S, Sattari G, Chelgani SC, Aliabadi M (2010) Prediction of uniaxial compressive strength and modulus of elasticity for Travertine samples using regression and artificial neural networks. Mining Sci Techn 20:41–46
Ebrahimi E, Monjezi M, Khalesi MR, Armaghani DJ (2015) Prediction and optimization of back-break and rock fragmentation using an artificial neural network and a bee colony algorithm. Bull Eng Geol Environ 75:27–36
Eftekhari M, Baghbanan A, Hashemolhosseini H (2015a) Fracture propagation in a cracked semicircular bend specimen under mixed mode loading using extended finite element method. Arabian J Geosci 8(11):9635–9646
Eftekhari M, Baghbanan A, Hashemolhosseini H, Amrollahi H (2015b) Mechanism of fracture in macro-and micro-scales in hollow centre cracked disc specimen. J Cent South Univ 22(11):4426–4433
Eftekhari M, Baghbanan A, Mohtarami E, Hashemolhosseini H (2017) Determination of crack initiation and propagation in two disc-shaped specimens using the improved maximum tangential stress criterion. J Theor Appl Mech 55(2):469–480
Feng G, Kang Y, Meng T, Hu YQ, Li XH (2017) The influence of temperature on mode I fracture toughness and fracture characteristics of sandstone. Rock Mech Rock Eng 50(8):2007–2019
Franklin JA, Zongqi S, Atkinson BK, Meredith PC, Rummel F, Mueller W, Nishimatsu Y, Takahahsi H, Costin LS, Ingraffea AR, Bobrov GF (1988) Suggested methods for determining the fracture toughness of rock. Int J Rock Mech Min Sci Geomech Abstr 25(2):71–96
Friedman JH (1991) Multivariate adaptive regression splines. Ann Stat 19(1):1–67
Guo H, Aziz NI, Schmidt LC (1993) Rock fracture-toughness determination by the Brazilian test. Eng Geol 33(3):177–188
ISRM (1988) Suggested methods for determining the fracture toughness of rock. Int J Rock Mech Min Sci Geomech Abstr 25(2):71–96
Jing L (2003) A review of techniques, advances and outstanding issues in numerical modelling for rock mechanics and rock engineering. Int J Rock Mech Min Sci 40:283–353
Kahraman S, Altindag R (2004) A brittleness index to estimate fracture toughness. Int J Rock Mech Min Sci 41(2):343–348
Ke CC, Chen CS, Tu CH (2008) Determination of fracture toughness of anisotropic rocks by boundary element method. Rock Mech Rock Eng 41(4):509–538
Kuruppu MD, Obara Y, Ayatollahi MR, Chong KP, Funatsu T (2014) ISRM suggested method for determining the mode I static fracture toughness using semi-circular bend specimen. Rock Mech Rock Eng 47(1):267–274
Lawal AI, Kwon S (2021) Application of artificial intelligence in rock mechanics: an overview. J Rock Mech Geotech Eng 13:248–266
Lawal AI, Kwon S (2022) Development of mathematically motivated hybrid soft computing models for improved predictions of ultimate bearing capacity of shallow foundations. J Rock Mech Geotech Eng. https://doi.org/10.1016/j.jrmge.2022.04.005
Lawal AI, Oniyide GO, Kwon S, Onifade M, Köken E, Ogunsola NO (2021) Prediction of mechanical properties of coal from non-destructive properties: A comparative application of MARS, ANN, and GA. Nat Resour Res 30:4547–4563
Mohammed DA, Alshkane YM, Hamaamin YA (2019) Reliability of empirical equations to predict uniaxial compressive strength of rocks using Schmidt hammer. Georisk Assess Manag Risk Engineered Sys Geohazards 14(4):308–319
Muñoz-Ibáñez A, Delgado-Martín J, Costas M, Rabunal-Dopico J, Alvarellos-Iglesias J, Canal-Vila J (2020) Pure mode I fracture toughness determination in rocks using a pseudo-compact tension (pCT) test approach. Rock Mech Rock Eng 53(7):3267–3285
Pakdaman AM, Moosavi M, Mohammadi S (2019) Experimental and numerical investigation into the methods of determination of mode I static fracture toughness of rocks. Theor Appl Fract Mech 100:154–170
Roy DG, Singh TN, Kodikara J, Talukdar M (2017) Correlating the mechanical and physical properties with mode-I fracture toughness of rocks. Rock Mech Rock Eng 50(7):1941–1946
Roy DG, Singh TN, Kodikara J (2018) Predicting mode-I fracture toughness of rocks using soft computing and multiple regression. Measurement 126:231–241
Sakellariou MG, Ferentinou MD (2005) A study of slope stability prediction using neural networks. Geotech Geol Eng 23:419–445
Wang W, Zhao Y, Teng T, Zhang C, Jiao Z (2021) Influence of bedding planes on mode I and mixed-mode (I–II) dynamic fracture toughness of coal: analysis of experiments. Rock Mech Rock Eng 54(1):173–189
Whittaker BN, Singh RN, Sun G (1992) Rock fracture mechanics: principles, design and application, vol 71. Elsevier Science Publishers, Amsterdam, p 591
Willmott CJ, Matsuura K (2005) Advantages of the mean absolute error (MAE) over the root mean square error (RMSE) in assessing average model performance. Climate Res 30(1):79–82
Xu C, Fowell RJ (1994) Stress intensity factor evaluation for cracked chevron notched Brazilian disc specimen. Int J Rock Mech Min Sci Geomech Abstr 31(2):157–162
Zhang Z (2002) An empirical relation between mode I fracture toughness and the tensile strength of rock. Int J Rock Mech Min Sci 39:401–406
Zhang Z, Kou S, Lindqvist P, Yu Y (1998) The relationship between the fracture toughness and tensile strength of rock. In: Yu M, Fan SC (eds) Strength theories: applications, development & prospects for 21st century. Science Press, Beijing, pp 215–219
Zhixi C, Mian C, Yan J, Rongzun H (1997) Determination of rock fracture toughness and its relationship with acoustic velocity. Int J Rock Mech Min Sci 34(3–4):491–4911